



Original Paper

Journal of Innovative Engineering
and Natural Science

(Yenilikçi Mühendislik ve Doğa Bilimleri Dergisi)

<https://dergipark.org.tr/en/pub/jieng>

Synthesis and application of soybean oil based photocurable polyurethane acrylates for aluminum coating

Berivan Ozer^a, Betül Nur Kus^a, Pelin Yetman^a, Müslüm Demircioğlu^a, Oguz Eryılmaz^a,
 Erhan Sancak^a, Zehra Yıldız^{a,*}

^aTextile Engineering, Marmara University, 34854, Istanbul, Turkey.

ARTICLE INFO

Article history:

Received 21 August 2024

Received in revised form 18 November 2024

Accepted 4 December 2024

Available online

Keywords:

Soybean oil
Photo curing
Metal coating
Spray coating
Carbamate ester

ABSTRACT

The aim of this work is to create a new bio-based photocurable oligomer by starting with soybean oil instead of petroleum-based chemicals. For this purpose, acrylic acid (AA) and epoxidized soybean oil (ESBO) were initially reacted. Then the obtained acrylated ESBO (AESBO) oligomer was reacted with the isocyanate groups of the 2,4-toluene diisocyanate - 2-hydroxyethyl methacrylate (TDI-HEMA) adduct. TDI was chosen as the isocyanate source since it is the most widely produced and used form of isocyanate in the global polyurethane industry. HEMA provided the hydroxyl and acrylate groups needed for UV curing and polyurethane production, respectively. Additionally, the oligomer is flexible due to the methyl side group of HEMA. The synthesized oligomer was characterized by Fourier transform infrared (FTIR) spectroscopy and differential scanning calorimetry (DSC) analysis. The coating compositions included the produced TDI-HEMA modified AESBO oligomer, as well as a variety of reactive diluents and a photoinitiator. Then formulations were applied on aluminum plates by spray coating and cured by UV light. The impact of the type of reactive diluent on the film forming and coating performance were all searched. Overall results proved that the inclusion of reactive diluents in the coating formulations helped to increase the coating quality and performance by adjusting the crosslinking density resulting in enhancement in adhesion.

I. INTRODUCTION

The degree of ductility or brittleness and crosslinking density of the coating material has a significant impact on a coating layer's resistance to scratches. Brittle coatings are more prone to damage or deformation when a force is applied to a coated substrate. It is possible to modify a coating material's brittleness and crosslinking density by designing an appropriate oligomer with the necessary capabilities. Because of their great chemical resistance, good adhesion, better abrasion resistance, durability, and toughness, polyurethanes are preferred in the coatings business. They work well in many applications such as footwear, adhesives, packaging materials, coatings, paints, heat insulators, foams, elastomers, biomedical items, and composites [1-3]. Polyols and diisocyanates, which give PU coatings their elastomeric qualities, are the building blocks of polyurethanes [4]. The high degree of crosslinking density between the isocyanate and hydroxyl groups gives polyurethane resins exceptional chemical resistance as well [5]. Utilizing photocuring technology, crosslinked polymeric structures are created by triggering a photochemical reaction with UV light. Following the degradation of photoinitiators by UV radiation, the photochemical reaction takes place in chemical species with unsaturated groups, such as vinyl ether, acrylate, etc. with free radicals. With UV-curing technology, the crosslinked structure is created in a matter of seconds, saving time, and the manufacturing process is ecologically beneficial since less or no solvent is utilized [6]. Furthermore, crosslinking is done at low temperatures, which has the financial benefit [7].

*Corresponding author. Tel.: +90-216-777-3980; e-mail: zehra.yildiz@marmara.edu.tr

Two functional chemical species with a hydroxyl group (hydroxyethyl methacrylate, hydroxyethyl acrylate, etc.) and an isocyanate group (toluene diisocyanate, isophorone diisocyanate, etc.) can react to create photocurable polyurethane acrylates. It is possible to construct polyurethane acrylates with specific qualities by varying the stoichiometry of the hydroxyl and isocyanate functionalities. A popular technique for creating UV-curable oligomer/polymer structures is the toluene diisocyanate-hydroxyethyl methacrylate (TDI-HEMA) reaction. In the TDI-HEMA adduct, HEMA provides the photocurable acrylate functionality that gives the oligomer flexibility, while TDI provides the isocyanate groups that give the oligomer its stiffness and hardness [8]. The -OH groups of HEMA react first with the isocyanates at para-positions during the synthesis of the TDI-HEMA adduct. The reactivity preference between the isocyanates in para- and ortho-positions can be explained by the variations in reactivity. Compared to isocyanates in para-position, those in ortho-position exhibit four times lower reactivity. In order to facilitate subsequent reactions, the isocyanates in ortho-positions are purposefully left unreacted [9]. Many researchers are searching for plentiful, affordable, non-toxic, biodegradable, and renewable plant-based replacements for polyols derived from petrochemicals [10-17], which are used in the synthesis of PU. When it comes to polymer synthesis, vegetable oils offer a viable substitute for petroleum-based starting monomers [18]. Soybean oil is the preferred vegetable oil because of its five unsaturated groups, which enable certain functional groups to react with it. According to the literature, the most popular method for modifying soybean oil is the epoxidation reaction, which is carried out with the help of a catalyst and hydrogen peroxide. The oligomer can then be given the required functionality by reacting with amines, acids, etc. on the produced oxirane ring on the soybean oil structure [4]. This study's primary goal is to synthesize a novel bio-based photocurable oligomer using soybean oil as a starting material rather than chemicals derived from petroleum. In order to achieve this, epoxidized soybean oil (ESBO) will first react with acrylic acid (AA). The resulting acrylated ESBO, or AESBO, will then undergo an additional reaction with the NCO groups of the TDI-HEMA adduct in an orthogonal configuration. Since TDI is the most produced and often utilized isocyanate type in the worldwide polyurethane sector, it was selected as the isocyanate source. HEMA was used as a source of hydroxyl and acrylate groups, respectively, to enable UV curing and polyurethane synthesis. In addition, the methyl side group of HEMA provides the oligomer with flexibility. The synthesized TDI-HEMA-modified AESBO oligomer was used in the coating formulations along with various types of reactive diluents and photoinitiators. The effects of the reactive diluent type on the coating performance and film forming properties were discussed.

II. EXPERIMENTAL METHOD

2.1 Materials

Tetrahydrofuran (THF, non-reactive diluent), photo initiator (1-hydroxycyclohexyl phenyl ketone, Irgacure® 184), epoxidized soybean oil (ESBO) (MW=952 g/mole, EEW=232 g/equiv.), 1,6-hexanediol diacrylate (HDDA, reactive diluent), N-vinylpyrrolidone (NVP, reactive diluent), trimethylolpropane triacrylate (TMPTA, reactive diluent), hydroquinone (HQ, inhibitor), dibutyltin dilaurate (T12, catalyst), acrylic acid (AA), 2,4-toluene diisocyanate (TDI), 2-hydroxyethyl methacrylate (HEMA), triphenyl phosphine (TPP, catalyst), sodium hydroxide (NaOH), were all obtained from Merck and used without any purification.

2.2 Synthesis of the TDI-HEMA Modified AESBO Oligomer

Figures 1, 2, and 3 are all showing the synthesis scheme of the proposed functional oligomer. In this study, the proposed oligomer is different from those of earlier research since it modifies soybean oil using the TDI-HEMA adduct. Figure 1 belongs to the synthesis scheme of the AESBO oligomer. During this reaction, a round-bottom flask, equipped with a nitrogen gas inlet, a condenser, and a magnetic stirrer were all used. The ESBO: AA molar ratio of 1:5 was set considering the epoxy equivalent weight (EEW) of ESBO (232 g/equiv.). At the beginning of the reaction, ESBO and HDDA (reactive diluent) (30% out of the total ESBO and AA amount) were loaded into

the glass flask. Another glass beaker was employed to dissolve HQ (300 ppm) and TPP (1000 ppm) in AA via ultrasonification. After the inclusion of the AA solution dropwise into the main flask, the reaction started to be heated at 100 °C for 2 h and 120 °C for 2 h. During the reaction, the depletion of AA was followed by the acid titration method, and the reaction was ended when a constant acid value (AV) of 8.25 mg KOH/g was observed. During the reaction, TPP initiated the reaction between the epoxide groups of ESBO and acid groups of AA by starting a nucleophilic attack resulting in the formation of phosphonium betaine. Following the attachment of an AA proton to the betaine, the carboxylate anion's action on the electrophilic carbon of the phosphorus created an ester bond (Figure 1a).

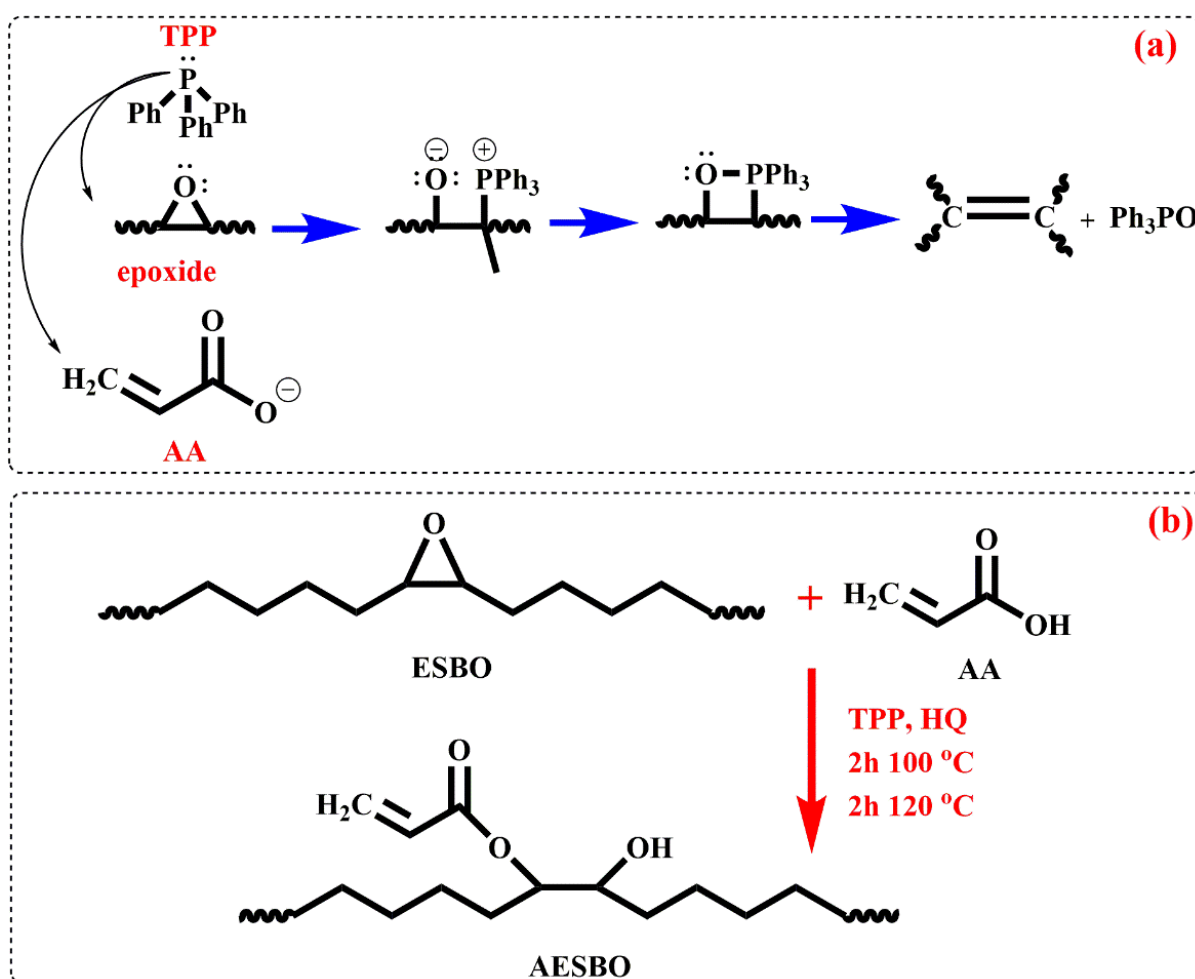


Figure 1. (a) Initiation reaction of TPP, (b) Synthesis scheme of the AESBO oligomer

In the second step, TDI-HEMA adduct was synthesized (Figure 2) to add urethane functional groups to the oligomer backbone. A round-bottom flask was employed having a magnetic stirrer and a condenser, for the synthesis reaction. The molar ratio of TDI:HEMA was set as 1:1 thus the one NCO group of TDI was intentionally left unreacted for further reaction with AESBO oligomer. At the beginning of the reaction, TDI along with THF (non-reactive diluent) were loaded into the flask, and then 0.03 wt% catalyst (T12) was added to the flask. Due to the sudden heat release, an ice bath was used, and HEMA was added dropwise to the main flask. After 30 min. of stirring in the ice bath, the reaction mixture was stirred at room temperature for another 30 min. Then the reaction proceeded at 70 °C for 1 h.

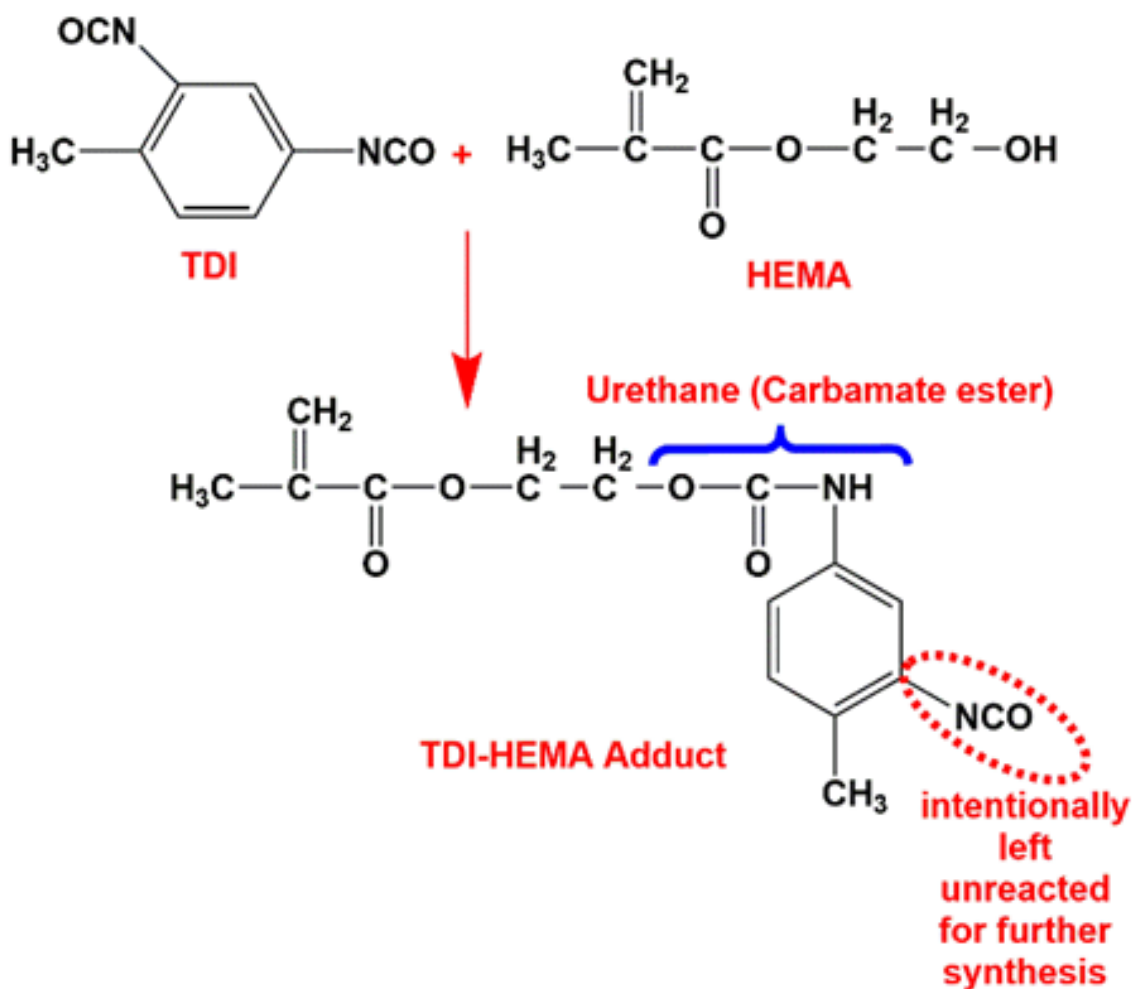


Figure 2. Synthesis scheme of the TDI-HEMA adduct

In the last step of the reaction, the -OH groups of AESBO oligomer which is formed by the epoxide ring opening reaction were reacted with the -NCO group of TDI-HEMA adduct. The scheme of this reaction can be followed in Figure 3. A certain amount of AESBO oligomer was mixed with the TDI-HEMA adduct by measuring the molar ratio of unreacted -NCO groups, in a round bottom flask having a magnetic stirrer and condenser. The reaction flask was heated to 80 °C for 1 h. The reaction ended when the isocyanate peak in FTIR spectra completely disappeared.

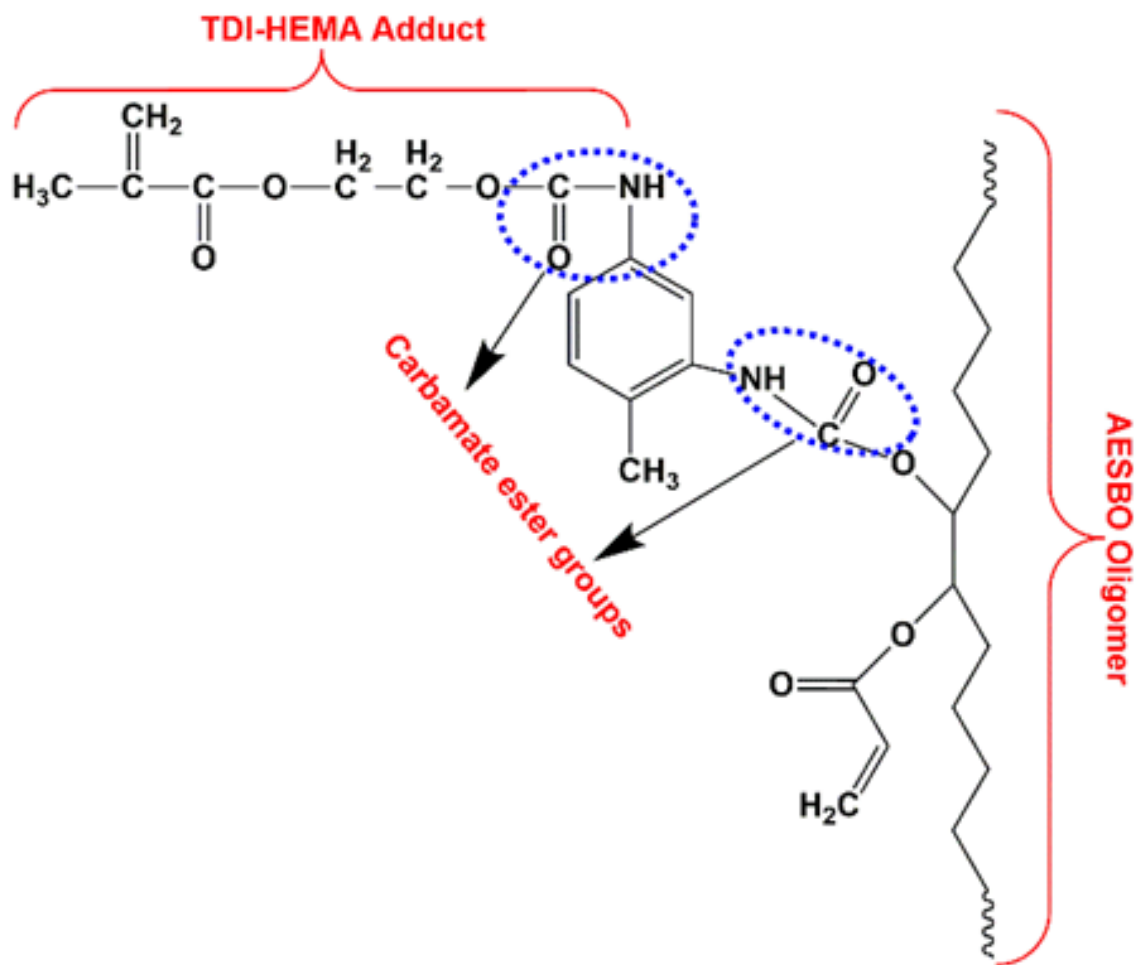


Figure 3. Synthesis scheme of the TDI-HEMA modified AESBO oligomer

2.2.1. Preparation and Application of Coating Formulations

The synthesized TDI-HEMA modified AESBO oligomer was included in the coating formulations along with 40 wt.% reactive diluent and 5 wt.% photoinitiator. Reactive diluents are frequently used in UV-curable coating formulations to reduce the formulation's viscosity and improve the coating layer's mechanical characteristics by adjusting the crosslinking density [21]. In this study, three different types of reactive diluents were employed to observe the effects of reactive diluent types on the coating performance of photo-cured TDI-HEMA modified AESBO oligomer. The type of the reactive diluent and the sample codes are illustrated in Table 1. After preparing the coating formulations, a spray gun (Figure 4a) was used to coat the Al surface. Then the coated surfaces were put in a zip-locked PE bag and two glass plates in order to prevent oxygen inhibition during photo-curing. A UV cabinet (Figure 4b), with a 365 nm UV light capacity, was used to cure the formulation.

Table 1. Sample codes and compositions

Sample Codes	Reactive Diluent	Functionality
A	None	None
B	NVP (N-vinylpyrrolidone)	Aromatic
C	HDDA (1,6-hexanediol diacrylate)	Difunctional
D	TMPTA (trimethylolpropane triacrylate)	Trifunctional

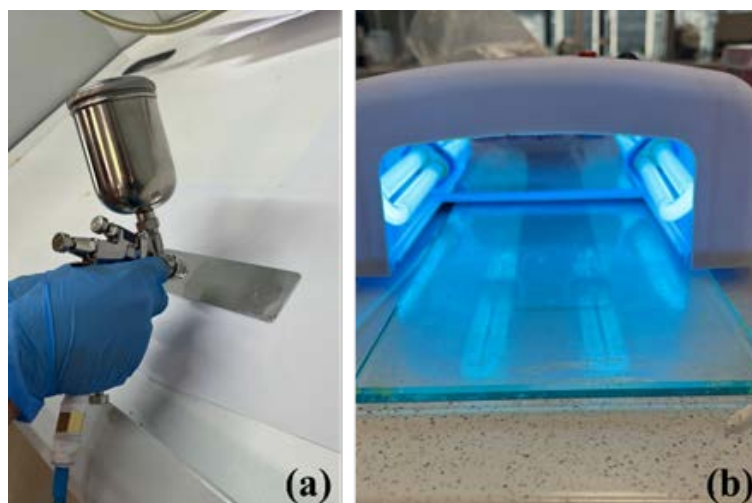


Figure 4. Spray coating (a) and UV-curing (b) processes

2.3. Characterization of materials

The synthesized oligomer was included in coating formulations along with the reactive diluents (Table 1) and photo initiator. Then, the formulations were casted on PTFE molds and cured by UV light to obtain UV-cured free films. Fourier transform infrared (FTIR, Perkin Elmer Spectrum 100 FTIR, with a ZnSe ATR sample holder) was used to analyze the chemical structure of the synthesized oligomers. Differential scanning calorimetry (DSC, Perkin Elmer Jade DSC instrument with Pyris software) was employed to observe the thermal transitions (T_g and T_d) of UV-cured free films. DSC analysis was recorded from 30-250 °C with a heating rate of 10 °C/min under a nitrogen atmosphere. The adhesion of coating formulations on Al plates was evaluated by using a cross-hatch (adhesion) test according to the DIN 53151 standard, by using a SH model of Sheen cross-cut testing kit. The coated UV-cured Al plates were also tested by means of rust formation upon water exposure by using the ASTM D610-08 standard.

III. RESULTS AND DISCUSSIONS

3.1 FTIR Analysis

The synthesized oligomers give characteristic peaks about the intended functional groups. The peak at 1744 cm^{-1} belongs to the carbonyl group of soybean oil for the spectra of a and b, whereas in c, it represents the carbonyl groups of HEMA and carbamate ester groups. The C-H asymmetric stretching vibration peaks in $-\text{CH}_2-$ and $-\text{CH}_3$ groups were observed at 2924 cm^{-1} and 2854 cm^{-1} , respectively. In the spectra of ESBO, the C-O-C asymmetric stretching vibration peaks at 823 cm^{-1} and 1155 cm^{-1} were attributed to the existence of the epoxide group. These peaks both disappeared after the reaction with AA. The newly formed peaks at 1619 cm^{-1} and 1636 cm^{-1} in AESBO spectra confirmed the existence of acrylate functionality with C=C double bond stretching vibration and C=O vibration. Additionally, the C-H bending vibration peak at 809 cm^{-1} also supports the epoxide ring-opening reaction. On the spectra of c and d, the carbonyl groups of HEMA and carbamate ester peaks at 1744 cm^{-1} overlap with the carbonyl group peaks of ESBO. Additionally, the peaks at $825\text{-}895\text{ cm}^{-1}$ region on the spectra of c and d,

are confirming that the existence of multiple substitution aromatic hydrocarbon units of TDI. The non-reactive diluent (THF) still exists in the system which needs to be evaporated prior to the coating and UV curing stages [19, 20].

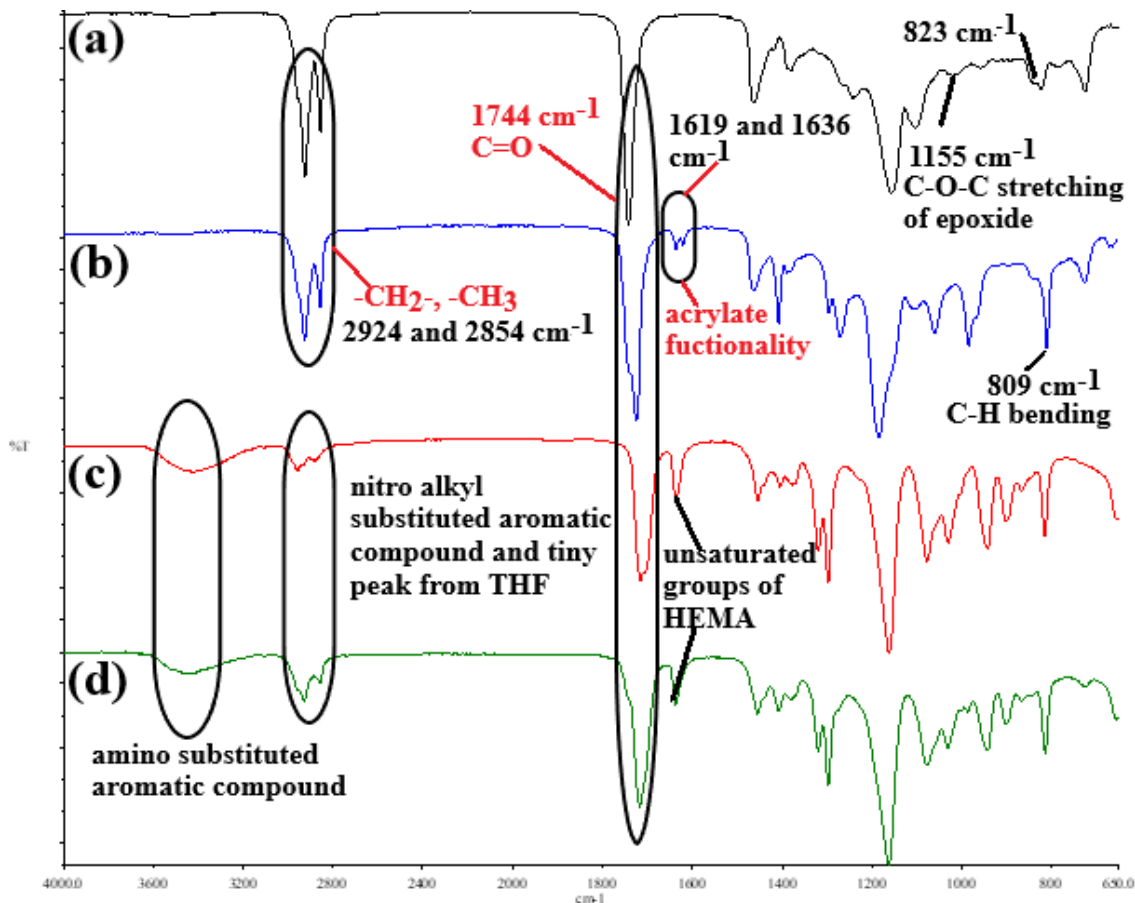


Figure 5. FTIR spectra of the synthesized oligomers; (a) ESBO, (b) AESBO, (c) TDI-HEMA adduct, (d) TDI-HEMA modified AESBO

3.2 DSC Analysis

DSC analysis was employed to observe the thermal transitions of UV-cured free films. Figure 6 shows the DSC curves of free films utilizing each reactive diluent type. The inclusion of reactive diluents in the formulation causes an increase in crosslinking density resulting in less molecular mobility with higher T_g values [21]. Accordingly, due to the bulky aromatic functional group of NVP, the sample of B showed the highest T_g value (102 °C). Considering samples C and D, having HDDA and TMPTA as reactive diluents, it is obvious that with the increasing functionality of the reactive diluents, T_g moves towards higher temperatures [22]. Thus, the T_g value of D is higher than C due to the trifunctional groups on its backbone. In other words, the decrease in T_g values can be explained by the following explanation; due to the penetration of reactive diluent molecules having shorter chains with less functionality between soybean oil-based oligomers, the chain alignment was disrupted and the van der Waals bonding between the adjacent chains were reduced thereby providing more free volume in the system. Besides T_g , the decomposition area was also observed in the 140-190 °C temperature range for all samples due to the inherent decomposition temperature of acrylate-based monomers around 180 °C [23, 24].

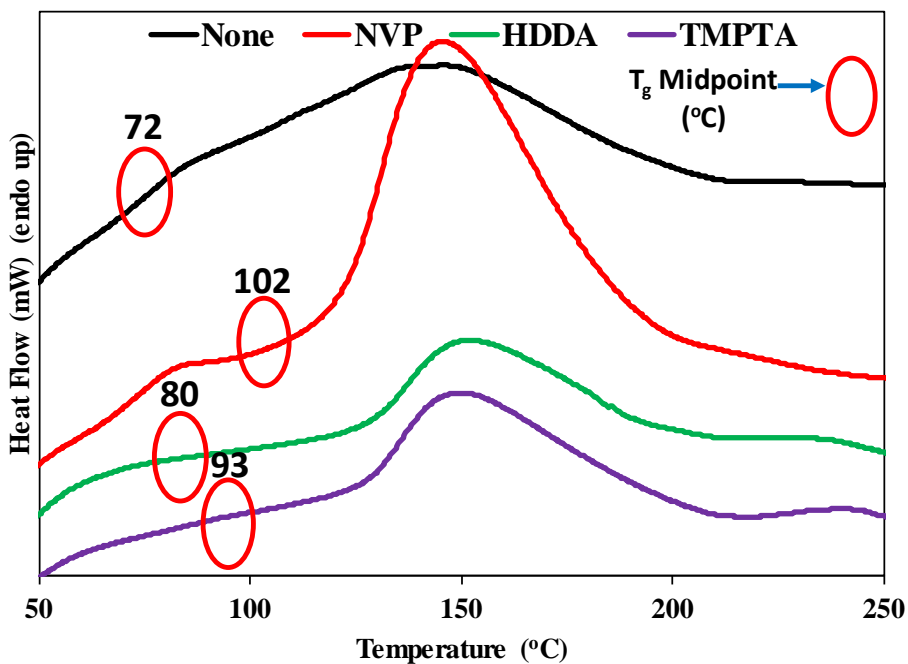


Figure 6. DSC curves of UV-cured free films

3.3 Crosscut Adhesion Test

The ASTM standard was followed for performing the cross-hatch (adhesion) test. The cross-hatch test result varies between 1B and 5B, where 1B denotes poor adhesion, which means that 35–65% of the film is taken from the surface, and 5B shows no film pull-off, which indicates the highest level of adhesion [25]. Figure 7 shows the cross-hatch test results along with the sample surface images. The sample A shows the poorest adhesion with a cross-hatch result of 2B. This result stems from the lack of reactive diluent in the formulation. After adding reactive diluents, the adhesion of the coating layer remarkably increased for all samples. The polar nature of acrylate groups in HDDA and TMPTA which support adhesion promotion caused the best cross-hatch test results with 4B in samples C and D. In contrast, in the sample of B, the pyrrolidone group of NVP has less polarity resulting in a less adhesion onto the Al surface.

3.4. Water Immersion Test

Table 2 shows the water immersion testing results of coated and UV-cured Al plates based on the visual evaluation of rusted areas after 24h water immersion. During the evaluation, rusted areas are categorized into 3 groups in terms of the shape and type of rusting. These are spot (S), pinpoint (P), and hybrid (H). In this study, after 24h water immersion of Al plates, rusting areas were observed in both spots and pinpoint shapes, thus a hybrid-type rusting occurred. Grading varies from 0 to 10 and 10 means no rusting, and 0 means more than 50% rusting. The testing result is given with both the grade and the type of rusting, i.e. 8-P means the rusted area is in the range of 0.03-0.1 % with a pinpoint rusting shape. Accordingly, the highest rusting grade of 3-H, which means that the rusted area is in the range of 10-16 % with a hybrid rusting shape, was recorded in the sample of A due to the lack of reactive diluent in the formulation resulting in poor adhesion on the surface. It is obvious that the inclusion of reactive diluent to the formulation helped to prevent the formation of rust by increasing the crosslinking density

resulting in enhancement in adhesion onto the surface. It seems that trifunctional and aromatic functional reactive diluents are much more effective than difunctional ones in preventing rusting [26].

Table 2. Water immersion testing results

Sample Codes			
None	NVP	HDDA	TMPTA
3-H	7-H	5-H	6-H
Scale and Type of Rusting			

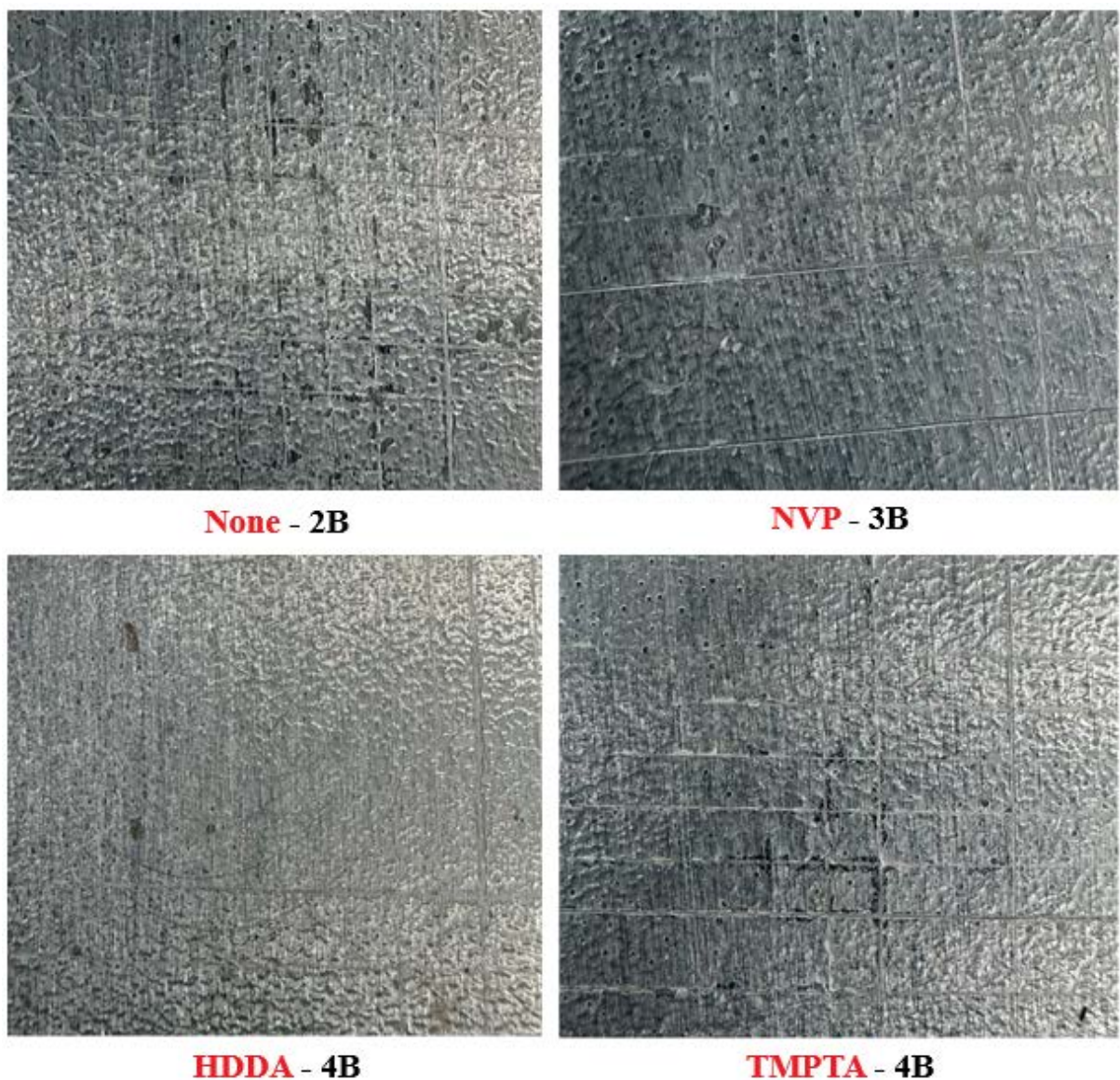


Figure 7. Cross cut testing results with the surface images

IV. CONCLUSIONS

In this study, a bio-based alternative to the petrochemical coating formulations on Al plates was examined with the help of UV-curing technology. The epoxide groups of ESBO were reacted with AA, and then the NCO groups of TDI-HEMA adduct were employed to modify the AESBO oligomer. The obtained photocurable oligomer was included in coating formulations with various reactive diluent types. FTIR spectra proved the formation of acrylic

functional groups in the AESBO oligomer backbone. The formation of carbamate ester groups upon the reaction with TDI-HEMA adduct was also followed by the FTIR spectroscopy. Due to the increase in crosslinking density with reactive diluents, T_g values shifted to the higher temperatures. The crosscut adhesion and water immersion test results revealed that the inclusion of reactive diluents in the coating formulations helped to increase crosslinking density resulting in enhancement in adhesion through giving less rusted areas. The number of functional groups of reactive diluents is the key parameter that determines the coating quality and performance. Besides, the type of functional group (aliphatic, aromatic, etc.) is also effective in coating quality by adjusting the free volume and molecular mobility of the polymer network. As conclusion, this study proved that bio-based photocurable formulations can be suggested as an alternative to the petrochemical components in conventional metal coating applications.

ACKNOWLEDGEMENT

This study was financially supported by TÜBİTAK İRA-SME project with the grant number “122N399”. The extended abstract of this study was orally presented at 14th International Fiber and Polymer Research Symposium (ULPAS), Bursa, Turkey, on 24-25th May, 2024.

REFERENCES

1. Boisaubert P, et al (2020) Photo-crosslinked coatings from an acrylate terminated non-isocyanate polyurethane (NIPU) and reactive diluent. *European Polymer Journal* 138, 109961. <https://doi.org/10.1016/j.eurpolymj.2020.109961>
2. Choi WC, et al (2023) Study on Press Formability and Properties of UV-Curable Polyurethane Acrylate Coatings with Different Reactive Diluents. *Polymers* 15(4), 880. <https://doi.org/10.3390/polym15040880>
3. Wang X, Soucek MD (2013) Investigation of non-isocyanate urethane dimethacrylate reactive diluents for UV-curable polyurethane coatings. *Progress in Organic Coatings* 76(7-8):1057-1067. <https://doi.org/10.1016/j.porgcoat.2013.03.001>
4. Alam M, et al (2014) Vegetable oil based eco-friendly coating materials: A review article. *Arabian Journal of Chemistry* 7(4):469-479. <https://doi.org/10.1016/j.arabjc.2013.12.023>
5. Das A, and Mahanwar P (2020) A brief discussion on advances in polyurethane applications. *Advanced Industrial and Engineering Polymer Research* 3(3):93-101. <https://doi.org/10.1016/j.aiepr.2020.07.002>
6. Park JW, et al (2018) Evaluation of UV curing properties of mixture systems with differently sized monomers. *Materials* 11(4):509. <https://doi.org/10.3390/ma11040509>
7. Wang S, et al (2020) Making organic coatings greener: Renewable resource, solvent-free synthesis, UV curing and repairability. *European Polymer Journal* 123:109439. <https://doi.org/10.1016/j.eurpolymj.2019.109439>
8. Yan Z, et al (2013) Synthesis and properties of a novel UV-cured fluorinated siloxane graft copolymer for improved surface, dielectric and tribological properties of epoxy acrylate coating. *Applied surface science* 284:683-691. <https://doi.org/10.1016/j.apsusc.2013.07.156>
9. Wang SJ, et al (2012) Preparation of polyurethane-poly (butyl acrylate) hybrid latexes via miniemulsion polymerization. *Applied Mechanics and Materials* 204:3938-3941. <https://doi.org/10.4028/www.scientific.net/AMM.204-208.3938>
10. Eryilmaz O (2024) Revalorization of cellulosic fiber extracted from the waste stem of Brassica oleracea var. botrytis L. (cauliflower) by characterizing for potential composite applications. *International Journal of Biological Macromolecules* 266:131086. <https://doi.org/10.1016/j.ijbiomac.2024.131086>
11. Eryilmaz O, Kocak ED, and Sancak E (2023) Braided natural fiber preforms, In: Midani M (ed) *Multiscale Textile Preforms and Structures for Natural Fiber Composites*, Woodhead Publishing, Manchester UK, pp 221-237. <https://doi.org/10.1016/B978-0-323-95329-0.00007-7>
12. Eryilmaz O, et al (2020) Investigation of the Water-Based Ink Hold onto the Thermoplastic Composites Reinforced with Sisal Fibers. *Journal of Textile Science Fashion Technology* 5(3). <https://dx.doi.org/10.33552/JTSFT.2020.05.000612>

13. Eryılmaz O, and Ovalı S (2024) Investigation and Analysis of New Fiber from *Allium fistulosum* L. (Scallion) Plant's Tassel and its Suitability for Fiber-Reinforced Composites. *Uludağ University Journal of The Faculty of Engineering* 29(1):51-66. <https://doi.org/10.17482/uumfd.1410520>
14. Ovalı S, and Eryılmaz O (2024) Physical and Chemical Properties of a New Cellulose Fiber Extracted from the *Mentha pulegium* L. (Pennyroyal) Plant's Stem. *Çukurova University Journal of The Faculty of Engineering* 39(1):211-220. <https://doi.org/10.21605/cukurovaumfd.1460444>
15. Ovalı S, Eryılmaz O, and Uyanık S (2024) Exploring the potential of sustainable natural cellulosic fiber from *Sorghum bicolor* (*Sorghum vulgare* var. *technicus*) stem for textile and composite applications. *Cellulose* 31(5):3289-3302. <https://doi.org/10.1007/s10570-024-05800-4>
16. Yildiz Z, and Eryılmaz O (2023) Preimpregnated natural fiber preforms, In: Midani M (ed) *Multiscale Textile Preforms and Structures for Natural Fiber Composites*, Woodhead Publishing, Manchester, UK, pp 327-340. <https://doi.org/10.1016/B978-0-323-95329-0.00003-X>
17. Yildiz Z, et al (2024) Sustainable fabric printing by using pre-consumed cellulosic textile wastes: The effect of waste particle content. *Journal of Cleaner Production* 448:141635. <https://doi.org/10.1016/j.jclepro.2024.141635>
18. Islam MR, Beg MDH, and Jamari SS (2014) Development of vegetable-oil-based polymers. *Journal of applied polymer science* 131(18). <https://doi.org/10.1002/app.40787>
19. Yildiz Z (2022) Usage of UV-Curable Soybean Oil Based Coating Formulations for Pretreated Cotton Fabrics. *Textile and Apparel* 32(3):232-242. <https://doi.org/10.32710/tekstilvekonfeksiyon.940434>
20. Yildiz Z, et al (2018) Effects of NCO/OH ratio and reactive diluent type on the adhesion strength of polyurethane methacrylates for cord/rubber composites. *Polymer-Plastics Technology and Engineering* 57(10):935-944. <https://doi.org/10.1080/03602559.2017.1364382>
21. Yildiz Z, and Onen HA (2017) Dual-curable PVB based adhesive formulations for cord/rubber composites: The influence of reactive diluents. *International Journal of Adhesion and Adhesives* 78:38-44. <https://doi.org/10.1016/j.ijadhadh.2017.06.004>
22. Wang F, Hu J, and Tu W (2008) Study on microstructure of UV-curable polyurethane acrylate films. *Progress in Organic Coatings* 62(3):245-250. <https://doi.org/10.1016/j.porgcoat.2007.12.005>
23. Goswami A, Umarji A, and Madras G (2010) Degradation kinetics of poly (HDDA-co-MMA). *Journal of applied polymer science* 117(4):2444-2453. <https://doi.org/10.1002/app.32122>
24. Li Q, et al (2016) Thermal degradation kinetics of poly (acrylate/ α -methyl styrene) copolymers. *Polymer Degradation and Stability* 128:158-164. <https://doi.org/10.1016/j.polymdegradstab.2015.10.003>
25. Dehmen OG, et al (2021) Synthesis and characterization of UV-curable cellulose acetate butyrate-based oligomers and their cotton fabric coatings. *Journal of Coatings Technology and Research* 18:1075-1085. <https://doi.org/10.1007/s11998-021-00461-5>
26. Goodarzi IM, et al (2014) Eco-friendly, acrylic resin-modified potassium silicate as water-based vehicle for anticorrosive zinc-rich primers. *Journal of applied polymer science* 131(12). <https://doi.org/10.1002/app.40370>